Materials Science and Engineering B 166 (2010) 46–49

Contents lists available at ScienceDirect

Materials Science and Engineering B

journal homepage: www.elsevier.com/locate/mseb

Photoluminescence studies of InAs/GaAs quantum dots covered by InGaAs layers

G.W. Shu[a], J.S. Wang[a], J.L. Shen[a,*], R.S. Hsiao[b], J.F. Chen[b], T.Y. Lin[c], C.H. Wu[d], Y.H. Huang[d], T.N. Yang[d]

[a] Physics Department, Chung Yuan Christian University, Chung-Pei Rd., Chung-Li, Taiwan
[b] Electrophysics Department, National Chiao-Tung University, Hsin-Chu, Taiwan
[c] Institute of Optoelectronic Sciences, National Taiwan Ocean University, Keelung, Taiwan
[d] Institute of Nuclear Energy Research, Atomic Energy Council, Long-Tan, Taiwan

ARTICLE INFO

Article history:
Received 29 May 2009
Received in revised form 23 August 2009
Accepted 25 September 2009

Keywords:
InAs
Quantum dots
Photoluminescence

ABSTRACT

Photoluminescence (PL), PL excitation (PLE), and time-resolved PL were used to study effects of InGaAs layers on the optical properties of InAs/GaAs quantum dots (QDs). A rich fine structure in the excited states of confined excitons (up to $n = 4$ quantum states) was observed, providing useful information to study the quantum states in the InAs/GaAs QDs. A significant redshift of the PL peak energy for the QDs covered by InGaAs layers was observed, attributing to the decrease of the QD strain and the lowing of the quantum confinement.

1. Introduction

Semiconductor quantum dots (QDs) with dimensions smaller than the bulk exciton Bohr radius provide a nearly zero-dimensional system, where carrier confinement occurs in all spatial directions. The quantum confinement results in discrete electronic levels which can be tuned by varying the QD size. The self-assembled QDs grown by the Stranski–Krastanov method have been proposed as a promising way to fabricate high-quality QDs, providing peculiar optical properties such as high quantum yield, tunability, and thermal stability. Because of these optical properties, QDs have led to considerable applications in optoelectronic devices such as optical switches, light-emitting diodes, and lasers [1–3]. Recently, much interest has been devoted to the development of GaAs-based materials emitting in the telecommunication wavelengths around 1.3 and 1.55 μm. The self-assembled InAs/GaAs QDs on GaAs substrate emit a photoluminescence (PL) peak with wavelength typically around 1050 nm [4]. An effective method to achieve the 1.3 μm spectral region is to cover an InGaAs thin layer to the InAs/GaAs QDs [5,6]. The InAs/GaAs QDs covered by InGaAs layers can redshift the QD emission by reduction of the residual compressive strain, increment of QD size, strain-driven decomposition of the InGaAs layer, and lowing of the lateral confinement (barrier lowing) [5,7–11]. Although 1.3-μm InAs/GaAs laser can be implemented using this approach, the fundamental properties of the InAs/GaAs QDs covered by InGaAs layers are not well understood. For example, the InGaAs layers would affect the confined electron states and hydrostatic strain in InAs/GaAs QDs. The addition of InGaAs layers may also change the thickness and strain of wetting layers (WLs), which have been demonstrated to influence the electronic and optical properties of self-assembled InAs/GaAs QDs considerably [12]. Understanding the fundamental properties of the InAs/GaAs QDs covered by InGaAs layers not only offers a convenient way to clarify the nature of their structures, but also provides useful information for extending their applications to optical devices.

In this paper, the PL, PL excitation (PLE), time-resolved PL techniques have been used to investigate the optical properties of the InAs/GaAs QDs covered by InGaAs layers. The PLE results show that the InAs/GaAs QDs reveal a clear quantum confinement effect even the InGaAs layers are included. By comparing the QDs with and without the InGaAs layers, we find that inclusion of the InGaAs layers leads to reduction of the WL thickness, decrease of the strain in WL and InAs QDs, and increase of the PL decay time.

2. Experimental details

The investigated structures in this study were grown by solid source molecular beam epitaxy (SS MBE) in a Riber Epineat machine on n^+-GaAs (100) substrates. The structure of InAs/GaAs QDs

* Corresponding author. Tel.: +886 32653227; fax: +886 32653299.
E-mail address: jlshen@cycu.edu.tw (J.L. Shen).

0921-5107/$ – see front matter © 2009 Elsevier B.V. All rights reserved.
doi:10.1016/j.mseb.2009.09.028

(without InGaAs layers) consists of a 3-nm-thickness AlAs bottom cladding layer, 10 stacks of InAs/GaAs QDs active region with 30-nm-thick GaAs barrier layer, a 3-nm-thickness AlAs top cladding, and a 10-nm-thick GaAs cap layer. QDs were formed in Stranski–Krastanow growth mode by the deposition of 2.6 monolayers (MLs) of InAs at substrate temperature of 485 °C, then covered with 10-nm-thick GaAs layer at the same temperature while the growth temperature of the rest layers was 600 °C. The structure of the other InAs/GaAs QDs (the QDs covered by the InGaAs layers) consists of a $Al_{0.3}Ga_{0.7}As$ bottom cladding layer, 10 stacks of InAs/InGaAs/GaAs QDs active region with 30-nm-thick GaAs barrier layer, a 30-nm-thick AlAs top cladding, and a 10-nm-thick GaAs cap layer. QDs were formed by deposition of 2.6 MLs of InAs at substrate temperature of 485 °C, then covered with 5-nm thick $In_{0.15}Ga_{0.85}As$ quantum well and 5-nm-thick GaAs barrier layer at the same temperature while the growth temperature of the rest layers was 600 °C.

The samples were mounted in a cold-finger cryostat and the sample temperature can be tuned between 10 and 300 K. Time integrated PL and PL decay measurements were made using pulsed diode lasers operating at a wavelength of 635 nm. The diode laser produces light pulses with about 40 ps duration and a repetition rate of 1 MHz. PLE measurements were carried out from a tungsten halogen lamp in conjunction with a monochromator as the excitation source. The collected luminescence was directly projected into a spectrometer and then detected with a high-speed photomultiplier tube (PMT), cooled down to −60 °C. PL decay signals were measured using the technique of time-correlated single-photon counting (TCSPC) by a PC plug-in time-correlated counting card. The overall temporal resolution of the apparatus is of the order of 250 ps.

3. Results and discussion

The inset of Fig. 1 displays the 20-K PL spectra of InAs/GaAs QDs with and without an InGaAs layer. For the sample without InGaAs layers, the energy of main peak is centered at 1.055 eV, which is assigned to the ground state transition. The high-energy shoulder is attributed to the recombination from the first excited state transition. The narrow QD-PL peak (full width at half maximum (FWHM) = 30.6 meV) reflects reduced dot size fluctuations and good shape uniformity. When the QDs were capped with a 5-nm-thick $In_{0.15}Ga_{0.85}As$ overgrown layer, the ground state transition is enhanced and redshifts to 1.038 eV. The low-energy shift could be due to a decreasing strain inside the QD, an increasing effective QD size caused by the strain-driven decomposition of the InGaAs layer, and the lowing of the lateral confinement [7–11].

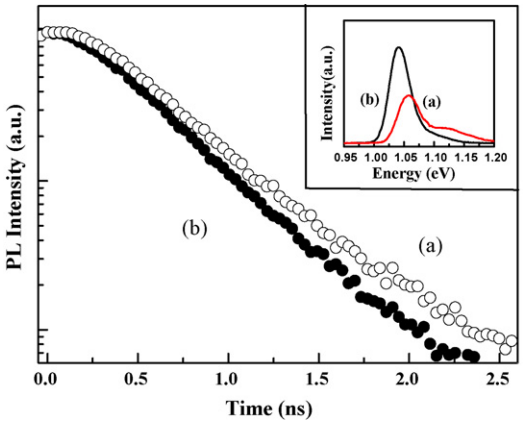

Fig. 1. The PL decay profiles monitored at ground state transition of the InAs/GaAs QDs (a) without and (b) with the InGaAs layers. The inset shows time integrated PL spectra of the InAs/GaAs QDs (a) without and (b) with the InGaAs layers at 20 K.

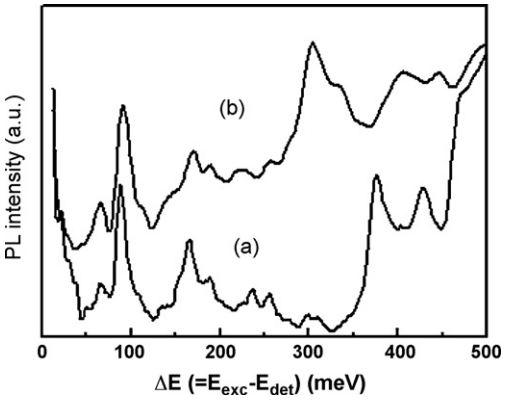

Fig. 2. The PLE spectra of the InAs/GaAs QDs (a) without and (b) with the InGaAs layers as a function of the excess excitation energy ($\Delta E = E_{exc} - E_{det}$). The detection energy E_{det} of (a) and (b) is 1.055 and 1.038 eV, respectively.

Fig. 1(a) and (b), respectively, displays the PL decay detected at the maxima of the ground state transition for QDs without and with InGaAs layers, revealing mono-exponential decays. The PL decay profiles of QDs were fitted to a single exponential function of the form $A_0 e^{-t/\tau 0}$ to extract a decay time τ_0. The decay curve gives time constant τ_0 of 0.48 and 0.43 ns for QDs without and with InGaAs layers, respectively. It has been reported that the QD shape in the InAs/GaAs QDs is pyramidal, leading to different elongation directions in the growth plane due to the macroscopic piezoelectric effect [8]. On the other hand, the shape of the InAs/GaAs QDs covered by InGaAs layers has been reported to be truncated pyramidal. The truncating pyramidal QDs weaken piezoelectric potential by the smaller side facets and shorter edges, and hence, the overlap of electron and hole wave functions increases. If we assume the radiative recombination process dominates the PL at low temperature (20 K), the shorter PL decay time for InAs QDs with InGaAs layers could be explained by the increased overlap for electron and hole wave functions when truncating the QDs.

Fig. 2(a) shows the PLE spectrum of the ground state transition, displayed with respect to the excess excitation energy ($\Delta E = E_{exc} - E_{det}$), for the InAs/GaAs QDs without the InGaAs layers. The sharp and discrete electronic transitions in the PLE spectrum demonstrate the high material quality and QD uniformity for the investigated sample. In order to understand the observed excitation resonances, a comparison with theoretical calculations is required. Based on an eight-band **k·p** model, calculations of the single-particle states in InAs/GaAs QDs have been carried out previously [13,14]. Since the pyramid base length of our QDs (∼18 nm) is comparable to the corresponding calculated value (17 nm) in Ref. [13], it is interesting to compare the PLE experiments with their theoretical calculations. If the quantum states are classified by the number of nodes in different directions [13,14], the absorption resonances in ΔE range between 50 and 110 meV in Fig. 2(a) can then be attributed to the transitions from valence band (VB) states |V100⟩ and |V010⟩ to the first excited conduction band (CB) states |C010⟩ and |C110⟩. Similarly, the absorption resonances between 130 and 210 meV are attributed to transitions from VB states |V020⟩ and |V200⟩ to CB states |C000⟩, |C300⟩, and |C020⟩. These line groups can thus be approximately assigned to the quantized levels of the two-dimensional harmonic oscillator and labeled as $n = 1, 2, \ldots$. Table 1 gives the absorption resonances measured from our PLE experiments and calculated from Ref. [13]. The good agreement between calculations and experiments suggests that the series of well-resolved excitation resonances are due to the quantum-size effect of the excited state spacing in InAs/GaAs QDs. In fact, we also observed some higher excited state transitions (ΔE between 280–325 meV) which have

Table 1
List of the absorption resonances of the InAs/GaAs QDs measured from PLE experiments and calculated from Ref. [13].

	Exciton transitions	ΔE(exp.) (meV)	ΔE(cal.) (meV)
$n=1$	$\|C100\rangle-\|V010\rangle$	65	67
	$\|C100\rangle-\|V110\rangle$	87	91
	$\|C010\rangle-\|V110\rangle$	107	105
$n=2$	$\|C020\rangle-\|V000\rangle$	135	142
	$\|C200\rangle-\|V300\rangle$	167	166

not been calculated in Ref. [13]. We deduce that those transitions can be assigned to $n=4$ transitions of confined excitons in QDs according to the model of two-dimensional harmonic oscillator. To our knowledge, our PLE spectra contain the clearest quantum-size effect in semiconductor QD structures so far. At higher photon energies, two intense absorption peaks positioned at $\Delta E=375$ and 430 meV are assigned to the heavy hole (HH) and light hole (LH) absorption of the WL, respectively. The heavy hole transition energy (1.430 eV) corresponds to a WL thickness of ~1 ML [15].

Fig. 2(b) shows the PLE spectrum of the ground state transition for InAs/GaAs QDs covered by InGaAs layers. For the absorption resonances below $\Delta E<350$ meV, it is found the spacing between the excited resonances increases after deposition of the InGaAs layers. For example, energy spacing of the $|C100\rangle-|V110\rangle$ ($|C200\rangle-|V300\rangle$) exciton transition increases from 87 (167) to 90 (172) meV. The increased energy spacing indicates that the quantum confinement effect is more pronounced as the InGaAs layers are included. In Fig. 2(b), additional absorption resonances positioned at $\Delta E=304$ and 333 meV are clearly observed and assigned to the HH and LH absorption of the InGaAs layers (quantum wells), respectively. The spacing of the HH and LH absorption of InGaAs layer, originating from the hydrostatic strain distribution in the growth direction, is predicated by calculations in the framework of continuum mechanics [8]. At higher energies, the peaks positioned at $\Delta E=405$ and 450 meV are, respectively, assigned to the HH and LH absorption of the WL. By comparing the QDs with and without InGaAs layers, the transition energies of WL shift to the higher energy side, indicating the effective WL thickness is reduced after the deposition of InGaAs layers. This reduction in the effective WL thickness may be due to the intermixing between the WL and InGaAs layers. It is noted that the strain-induced spacing of the HH and LH absorption of WL is found to decrease from 55 to 45 meV as the InGaAs layers are included. It has been recently reported that the strain profile in WL is almost identical to that in InAs QDs [12]. Therefore, the strain in WL region represents the strain within the InAs dots. The reduced strain-induced spacing of the HH and LH absorption of WL demonstrates a decrease of the hydrostatic strain within the QDs after the deposition of InGaAs layers.

Here, we try to discuss the origin of PL redshift in our case. According to continuum methods for strain calculations in QDs, the strain is proportional to the lattice mismatch between QDs and confining layer materials [16,17]. With covering the InGaAs (confining) layers, the lattice constants of InAs and InGaAs layers are not so much different compared to those of InAs and GaAs. Therefore, the QD strain decreases after covering an InGaAs layers. This reduced strain of QDs was considered as an important factor for redshift of the PL emission in QDs [5,17]. An effective-mass model of electronic transition in InAs/InGaAs QDs has been proposed for the development of QD strain engineering [18,19]. On the other hand, the quantum confinement effect may change with covering the InGaAs layers. The QD size may increase as the InGaAs layer is grown, especially in the growth direction [7,20]. The quantum-size effect of QDs in the growth direction is more pronounced than that in the other directions since the QD height is much smaller than the lateral size of QDs. Thus, the increase in QD height caused by

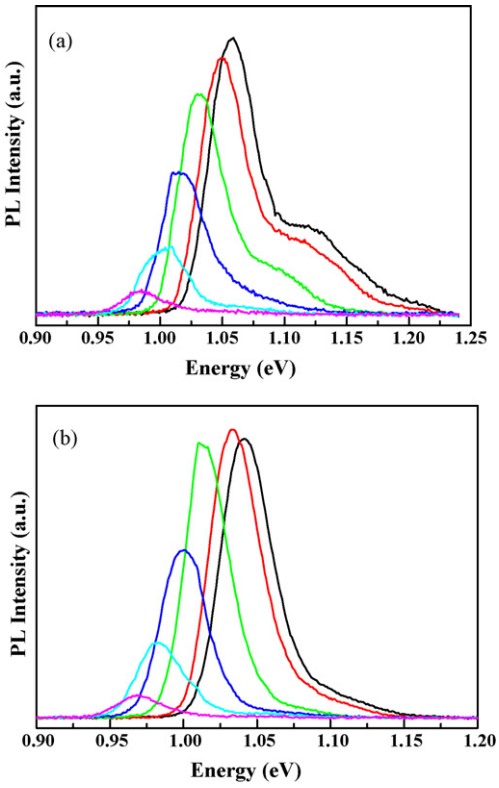

Fig. 3. The PL spectra of the InAs/GaAs QDs (a) without and (b) with the InGaAs layers recorded at $T=10$, 80, 140, 180, 220, and 260 K.

covering the InGaAs layers reduces the quantum confinement of QDs, producing the redshift in the PL peak. Additionally, the introduction of InGaAs layers decreases the barrier height in the band diagram, which causes a lowing of the lateral confinement. Also, the QD shape may affect the quantum confinement states in InAs/GaAs QDs. According to the eight-band **k·p** calculations, the ground state transition energy of the truncating pyramidal QDs (the QDs with InGaAs layers) is smaller than that of the pyramidal QDs (the QDs without InGaAs layers), having the same QD volume [21]. Therefore, truncating the QD shape can decrease the PL peak energy. From our PLE measurements (Fig. 2), the reduced spacing of the HH and LH absorption of WL indicates that the hydrostatic strain decreases for the QDs with InGaAs layers. We therefore deduce that the strain reduction effect plays an important role for the redshift in PL peak energy in the QDs with InGaAs layers. However, we cannot completely exclude the contribution of lowing of the quantum confinement, originating from the decrease of barrier height, the increase of QD height, and the change of QD shape. The redshift in the PL peak may, at least in part, originate from the effect of quantum confinement.

The PL spectra of QDs without and with InGaAs layers as a function of temperature are displayed in Fig. 3(a) and (b), respectively. Both spectra show the temperature dependence typical of an ensemble of QDs [22]. With increasing temperature, the PL band maximum shifts toward the low-energy side and the PL intensity decreases. The quenching of PL intensity with increasing temperatures can be accounted for by the increased nonradiative recombination of confined carrier loss, in competition with radiative recombination. The open circles in Fig. 4 show the integrated PL intensities as the function of the inverse of temperature for QDs without and with InGaAs layers. We extract the corresponding activation energy by using the following equation:

$$A(T)=\frac{A_0}{1+C\exp(-E_0/kT)}, \quad (1)$$

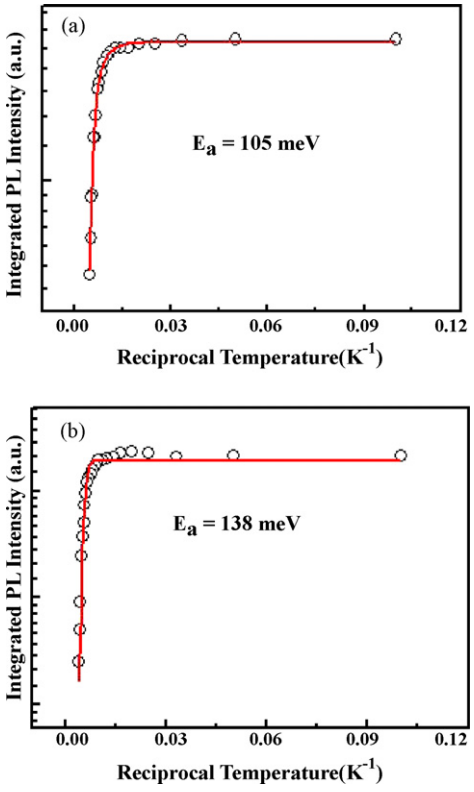

Fig. 4. The temperature dependence of integrated PL intensities of the InAs/GaAs QDs (a) without and (b) with the InGaAs layers. The solid lines are the calculated results using Eq. (1), from which the thermal activation energies are determined.

where A_0 is a constant, E_0 is the thermal activation energy, and k is the Boltzmann constant. The thermal activation energies for QDs without and with InGaAs layers are fitted to be 105 and 138 meV, respectively. The larger activation energy for QDs with InGaAs layers can be explained by the energy difference between the ground state and the WL. From PLE spectra of the ground state transition (Fig. 2), the excess excitation energy (ΔE) between the ground state and the WL is 375 and 405 meV for the QDs without and with the InGaAs layers, respectively. At elevated temperatures, the carriers in the ground state of the QDs with InGaAs layers are less efficient to be thermally populated to the WL, where carriers are lost irreversibly. Therefore, E_0 for the QDs with InGaAs layers is larger than that for the QDs without InGaAs layers.

4. Conclusions

We study PL properties of InAs/GaAs QDs without and with InGaAs layers using different PL techniques. A rich fine structure in the excited states (up to $n = 4$ quantum states) was observed in PLE studies, providing clear information to analyze the quantum confined states in the InAs/GaAs QD system. The inclusion of InGaAs layers shifts the PL emission of QDs toward the low-energy side. The redshift of the PL in InAs QDs was found to be associated with the reduction of the QD strain and the lowing of lateral confinement. The increased activated thermal energy after covering the InGaAs layers can be accounted for by the increased energy spacing between the ground state and the WL.

Acknowledgments

This project was supported in part by the National Science Council under the grant numbers NSC97-2112-M-033-004-MY3 and NSC 97-2627-B-033-002 and by the Institute of Nuclear Energy Research under the grant number 962001INER0041.

References

[1] D. Bimberg, M. Grundmann, N.N. Ledentsov, Quantum Dot Heterostructures, Wiley, New York, 1998.
[2] C.P. Collier, T. Vossmeyer, J.R. Heath, Annu. Rev. Phys. Chem. 49 (1998) 371.
[3] Y. Masumoto, T. Takagahara:, Semiconductor Quantum Dots, Springer, Berlin, 2002.
[4] M. Grundmann, N.N. Ledentsov, O. Stier, D. Bimberg, V.M. Ustinov, P.S. Kop'ev, Z.I. Alferov, Appl. Phys. Lett. 68 (1996) 979.
[5] K. Nishi, H. Saito, S. Sugou, J.–S. Lee, Appl. Phys. Lett. 74 (1999) 1111.
[6] V.M. Ustinov, N.A. Maleev, A.E. Zhukov, A.R. Kovsh, A.Y. Egorov, A.V. Lunev, B.V. Volovik, I.L. Krestinov, Y.G. Musikhin, N.A. Bert, P.S. Kop'ev, Z.I. Alferov, N.N. Ledentsov, D. Bimberg, Appl. Phys. Lett. 74 (1999) 2815.
[7] J.S. Kim, P.W. Yu, J.I. Lee, J.S. Kim, S.G. Kim, J.Y. Leem, M. Jeon, Appl. Phys. Lett. 80 (2002) 4714.
[8] F. Guffarth, R. Heitz, A. Schliwa, O. Stier, N.N. Ledentsov, A.R. Kovsh, V.M. Ustinov, D. Bimberg, Phys. Rev. B 64 (2001) 085305.
[9] F. Guffarth, R. Heitz, A. Schliwa, O. Stier, A.R. Kovsh, V. Ustinov, N.N. Ledentsov, D. Bimberg, Phys. Stat. Sol. B 224 (2001) 61.
[10] W.-H. Chang, H.Y. Chen, H.-S. Chang, W.-Y. Chen, T.M. Hsu, T.-P. Hsieh, J.-I. Chyi, N.-T. Yeh, Appl. Phys. Lett. 86 (2005) 131917.
[11] W.-S. Liu, J.-I. Chyi, J. Appl. Phys. 97 (2005) 024312.
[12] S. Lee, O.L. Lazarenkova, P. von Allmen, F. Oyafuso, G. Klimeck, Phys. Rev. B 70 (2004) 125307.
[13] R. Heitz, O. Stier, I. Mukhametzhanov, A. Madhukar, D. Bimberg, Phys. Rev. B 62 (2000) 11017.
[14] O. Stier, R. Heitz, D. Bimberg, Phys. Rev. B 59 (1999) 5688.
[15] M. Ilg, M.I. Alonso, A. Lehmann, K.H. Ploog, M. Hohenstein, J. Appl. Phys. 74 (1993) 7188.
[16] G.S. Pearson, D.A. Faux, J. Appl. Phys. 88 (2000) 730.
[17] L. Seravalli, M. Minelli, P. Frigeri, P. Allegri, V. Ananzini, S. Franchi, Appl. Phys. Lett. 82 (2003) 2341.
[18] L. Seravalli, P. Frigeri, M. Minelli, P. Allegri, V. Ananzini, S. Franchi, Appl. Phys. Lett. 87 (2005) 063101.
[19] L. Seravalli, M. Minelli, P. Frigeri, S. Franchi, G. Guizzetti, M. Patrin, T. Ciabattoni, M. Geddo, J. Appl. Phys. 101 (2007) 024313.
[20] H.Y. Liu, X.D. Wang, J. Wu, B. Xu, Y.Q. Wei, W.H. Jiang, D. Ding, X.L. Ye, F. Lin, J.F. Zhang, J.B. Liang, Z.G. Wang, J. Appl. Phys. 88 (2000) 3392.
[21] R. Heitz, Physica E 16 (2003) 68.
[22] S. Sanguinetti, M. Henini, M.G. Alessi, M. Capizzi, P. Frigeri, S. Franchi, Phys. Rev. B 60 (1999) 8276.